

Engraftment of Human Stem Cell-Derived Otic Progenitors in the Damaged Cochlea

Alejandra Lopez-Juarez,^{1,2} Hanae Lahlou,^{1,3} Chantal Ripoll,⁴ Yves Cazals,¹ Jean Michel Brezun,^{1,6} Quan Wang,³ Albert Edge,³ and Azel Zine^{1,5}

¹CNRS UMR 7260, Aix-Marseille Université, Marseille, France; ²Chemical, Electronic and Biomedical Engineering, Universidad de Guanajuato, Guanajuato, Mexico;

³Harvard Medical School, Massachusetts Eye and Ear Infirmary, Boston, MA, USA; ⁴Institute for Neurosciences of Montpellier, Inserm U1051, Montpellier, France;

⁵Laboratory of Bioengineering and Nanoscience, LBN, University of Montpellier, Montpellier, France

Most cases of sensorineural deafness are caused by degeneration of hair cells. Although stem/progenitor cell therapy is becoming a promising treatment strategy in a variety of organ systems, cell engraftment in the adult mammalian cochlea has not yet been demonstrated. In this study, we generated human otic progenitor cells (hOPCs) from induced pluripotent stem cells (iPSCs) *in vitro* and identified these cells by the expression of known otic markers. We showed successful cell transplantation of iPSC-derived-hOPCs in an *in vivo* adult guinea pig model of ototoxicity. The delivered hOPCs migrated throughout the cochlea, engrafted in non-sensory regions, and survived up to 4 weeks post-transplantation. Some of the engrafted hOPCs responded to environmental cues within the cochlear sensory epithelium and displayed molecular features of early sensory differentiation. We confirmed these results with hair cell progenitors derived from *Atoh1*-GFP mice as donor cells. These mouse otic progenitors transplanted using the same *in vivo* delivery system migrated into damaged cochlear sensory epithelium and adopted a partial sensory cell fate. This is the first report of the survival and differentiation of hOPCs in ototoxic-injured mature cochlear epithelium, and it should stimulate further research into cell-based therapies for treatment of deafness.

INTRODUCTION

Hearing loss and vestibular dysfunction are the most common sensory deficits in humans.¹ The inner ear is a highly specialized sensory organ containing auditory and vestibular hair cells (HCs) that transduce mechanical energy into electrical energy.² During otic development, HCs in the inner ear are derived from otic progenitors through a precise temporally and spatially coordinated pattern of gene expression orchestrated by complex signaling cascades.^{3,4} They are limited in number and are susceptible to damage from a variety of insults, ranging from ototoxic drugs to loud noise exposure, genetic mutations, or aging. In contrast to the avian cochlea, which is able to regenerate lost HCs,^{5,6} the mature mammalian cochlea is unable to spontaneously regenerate lost HCs, leading to permanent hearing loss.⁷ Adult-onset hearing loss ranks among the top five leading causes of disease burden in Europe, entailing enormous socioeconomic costs.⁸ Prosthetic treatment with hearing aids or cochlear

implants is limited, reaching only every fifth patient. When considering curative treatment options for hearing loss, two emerging approaches, both of which attempt to replace lost HCs, have been the subjects of interest: gene- and cell-based therapies.^{9–13} Regarding genetic hearing loss, several successful *in vivo* gene therapy treatments have been reported in embryonic and neonatal mouse inner ears, either through gene transfer or antisense oligonucleotide therapies.^{14–16} These studies report potential gene therapy strategies that partially promote vestibular and/or hearing recovery in mice.

While stem/progenitor cell transplantation therapy might also be a potential option for the treatment of hearing loss, only a few previous reports have described the use of *in vivo* cell transplantation therapy for inner ear sensory deficits. These studies used various cell types for transplantation into the inner ear, i.e., dorsal root ganglion cells,¹⁷ mouse embryonic stem cells,¹⁸ neural stem cells,^{19–21} mesenchymal stem cells,²² or adult olfactory stem cells.²³ However, no consensus has been reached as to the feasibility of a cell-based therapeutic approach in the inner ear or the optimal cell type or route of delivery for these studies. Additional investigations with pluripotent stem cells either from mouse²⁴ or human²⁵ origins principally focused on engraftment of embryonic stem cell-derived neural progenitors in the modiolus in an animal model of auditory neuropathy. In addition, human induced pluripotent stem cells (hiPSCs) obtained by cell reprogramming²⁶ have received considerable attention, as a cellular platform for the *in vitro* production of cell types of interest, including otic cells, by recapitulating their early developmental steps. Moreover, in the future, hiPSCs may serve as an autologous source of replacement for HCs and/or neurons in the injured inner ear, if the *in vitro* differentiation toward early otic lineage and further *in vivo* sensory cell differentiation post-grafting can be properly guided. Although several previous reports have described protocols for

Received 18 October 2018; accepted 26 March 2019;
<https://doi.org/10.1016/j.ymthe.2019.03.018>

⁶Present address: Aix-Marseille Université, UMR 7287, ISM, 13288 Marseille, France

Correspondence: Azel Zine, PhD, Laboratory of Bioengineering and Nanoscience, LBN, University of Montpellier, 545 rue du Prof. Viala, 34193 Montpellier Cedex 5, France.

E-mail: azel.zine@umontpellier.fr

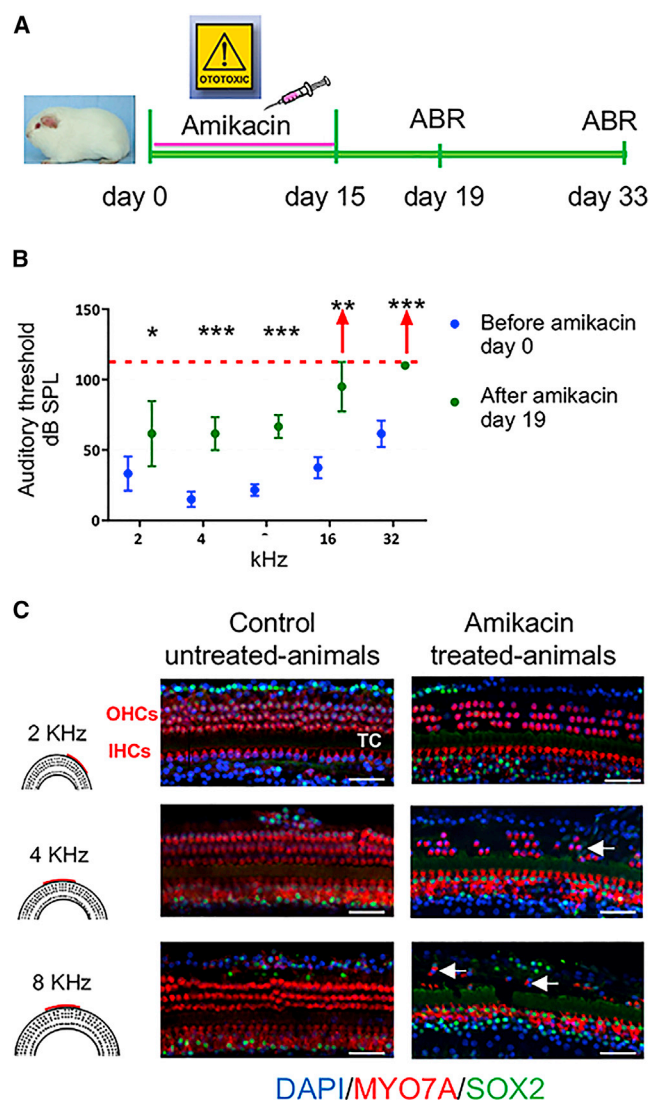


Figure 1. A Model of Ototoxic Trauma-Induced Sensori-Neural Hearing Loss

(A) Timeline of ototoxic drug lesion and electrophysiological measurements. (B) Auditory thresholds were measured by ABR. Pooled threshold values are represented by a dot ($n \geq 4$ per group) and the SD indicated by a bar. After amikacin exposure, the ABR measurements showed a threshold shift of at least 20 dB at all the frequencies tested. Red arrows represent animals with an auditory threshold greater than 90 dB for frequencies from 16 to 32 kHz. Wilcoxon rank-sum test * $p < 0.05$, ** $p < 0.01$, *** $p < 0.001$. (C) Confocal images of immunostaining for MYO7A (shown in red) and SOX2 (shown in green) on whole-mount surface preparations from second and basal cochlear turns (i.e., regions coding frequencies of 2, 4, and 8 kHz) of control-untreated and amikacin-treated animals. Amikacin exposure resulted in a severe loss of OHCs within the basal cochlear turn. Most of OHCs were missing, but a few MYO7A- and SOX2-immunopositive cells remained within the region of damaged cochlear sensory epithelium (arrows). Most of IHCs remain after amikacin treatment. IHCs, inner hair cells; OHCs, outer hair cells; TC, tunnel of Corti. Scale bars, 50 μm in all panels.

in vitro differentiation of human pluripotent stem cells to otic sensory derivatives,^{27–29} there have been no follow-up protocols for *in vivo* transplantation of human otic sensory cells in the adult mammalian inner ear. Currently, the approach for stem/progenitor cell transplantation in the adult inner ear revolves around generating a sufficient number of characterized human otic progenitor cells (hOPCs) *in vitro*, defining an appropriate delivery route, and promoting their survival, migration, and differentiation in the *in vivo* cochlear micro-environment.^{9,30}

This study represents the first attempt to explore the feasibility of hiPSC-derived hOPC transplantation into impaired adult mammalian cochlea after HC damage. To that end, we initially generated hOPCs from the induction of hiPSCs in a monolayer culture system and subsequently examined the *in vivo* engraftment of these partially differentiated hOPCs in adult guinea pig model of ototoxicity.

The results from our study are a proof of principle; that transplantation of iPSC-derived-hOPCs may be a useful therapeutic strategy to repair the damaged mammalian cochlea. The hOPCs used in this study migrated, incorporated into the ototoxin-exposed cochlear sensory epithelium, and partially differentiated into cells expressing initial HC and supporting cell markers.

RESULTS

Amikacin Ototoxicity and HC Loss in the Adult Guinea Pig

An ototoxic effect was induced by administration of amikacin for 15 days with one daily injection of amikacin at the dose of 400 mg/kg/day (Figure 1A). Auditory threshold was measured by auditory brain response (ABR) at basal levels (before starting treatment, day 0) and 4 days after the end of treatment (day 19). Amikacin-treated animals showed at least 20 dB threshold shift at all the frequencies tested and, in some cases (three of six animals), no response was detected even at 90 dB for 16 and 32 kHz coding frequencies (Figure 1B).

To characterize the pattern of HC loss induced by amikacin exposure in adult cochleae, we used immunostaining for MYO7A to identify surviving HCs. Whole-mount cochlear surface preparations were also double-labeled with SOX2 staining to visualize the supporting cells (Figure 1C). In control untreated animals, all MYO7A-immunopositive HCs, including one row inner HCs (IHCs) and three rows of outer HCs OHCs, were present in the cochlear sensory epithelium at the base, middle, and apical regions. Parallel histological analyses of cochleae from animals treated with amikacin revealed a minor loss of OHCs at the region coding 2 kHz, increasing to virtually complete loss of OHCs at regions encoding the frequencies of 8, 16, and 32 kHz (basal cochlear turn). Some OHCs remain localized at the basal cochlear turn, while the IHCs remained intact in the whole cochlea following amikacin (400 mg/kg/day for 15 days) exposure. Surprisingly, in animals treated with amikacin, SOX2 signal was observed in the remaining MYO7A-immunopositive HCs mostly at 4 and 8 kHz regions. This expression of SOX2 in HCs appears to be different from its known specific expression in supporting cells in normal and drug-damaged

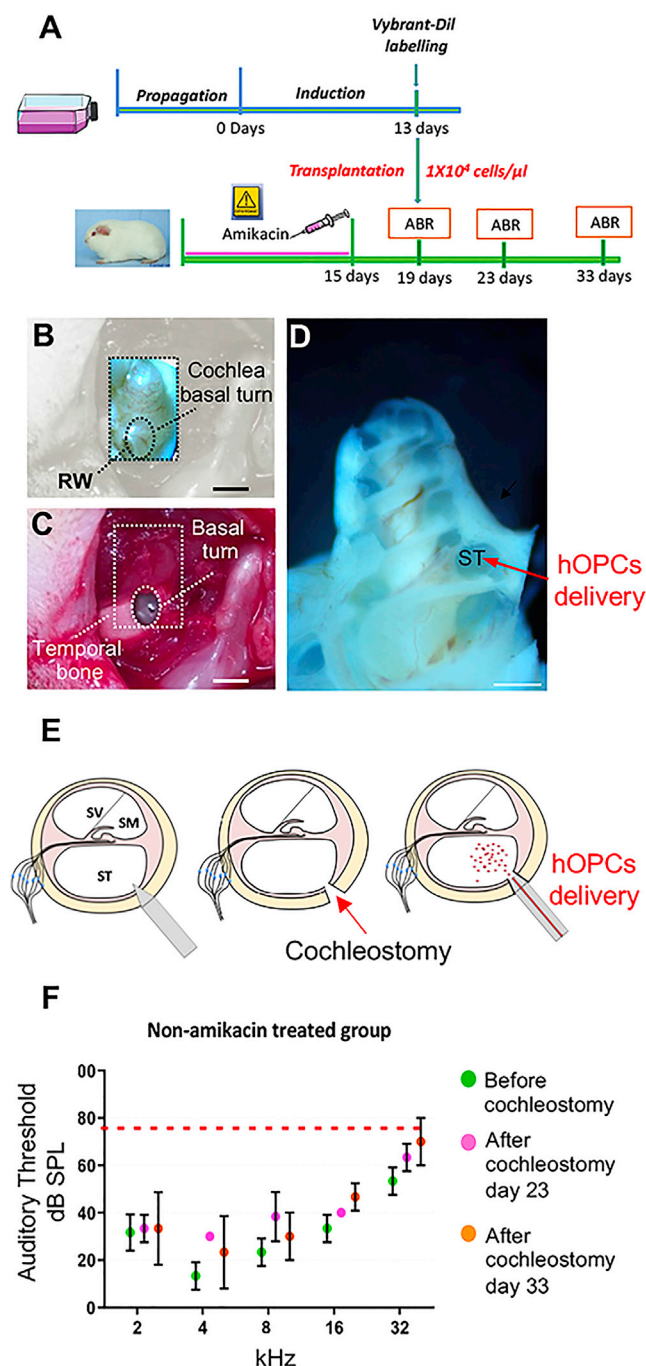


Figure 2. Surgical Approach for Cell Injection into the Scala Tympani

(A) Timeline of human iPSC-derived otic progenitors *in vitro* and *in vivo* transplantation in adult guinea pig model of ototoxicity. (B–D) The anatomical landmarks used to ensure that the site of cochleostomy was consistent between animals are shown. A cochleostomy was performed at the base of the cochlea; dashed box in (B) and (C) and red arrow in (D) driving the cells into the scala tympani. (E) Schematic representation of sequential steps to inject hOPCs into the scala tympani by cochleostomy. (F) ABR measurements were performed on amikacin-untreated animals before cochleostomy (D19), 4 days after cochleostomy (D23), and 14 days after cochleostomy (D33). Auditory threshold values of

adult mouse inner ears.³¹ However, in the same study, SOX2 expression was detected in a subset of vestibular HCs in the mouse inner ear. At present, it is difficult to speculate regarding this difference between drug-exposed adult mouse and guinea pig models as well as to the role of SOX2 in guinea pig HCs following amikacin exposure.

Our aminoglycoside ototoxicity model generated an experimental paradigm to eliminate many OHCs in the organ of Corti of adult guinea pig *in vivo* that we used to investigate the transplantation of hiPSC-derived hOPCs. The loss of OHCs is the most prevailing neurosensory loss in aging humans, making our model an appropriate test model for the treatment of age-related human hearing loss.

Surgical Approach for Otic Progenitor Transplantation into the Cochlea

The success of transplantation depends on surgical techniques designed to ensure precise cell injection while minimizing surgical trauma and hearing loss. We were particularly interested in routing engrafted cells within amikacin exposed-cochlear sensory epithelium, which is surrounded by two compartments: the scala media and scala tympani. The high level of potassium (150 mM) present in the endolymphatic compartment constitutes a hostile environment for engrafted cells in the scala media of the cochlea.^{32,33} In contrast, when the cells are delivered into the scala tympani, some are able to migrate to the scala media and vestibuli.^{20,34} Furthermore, the scala tympani can be easily reached by cochleostomy via a post-auricular approach with minor inflammatory responses.³⁵ In this work, we adapted the cochleostomy procedure described by Backhouse et al.³⁶ to ensure minimally invasive access to the cochlea and efficient delivery of hOPCs into the scala tympani (Figures 2A and 2D). The auditory threshold of untreated or amikacin-treated animals undergoing cochleostomy was not affected by the cochleostomy as indicated by ABR before surgery (i.e., day 19), 4 days (i.e., day 23), and 14 days post-surgery (i.e., day 33) (Figures 2F and S1).

In Vitro Differentiation of hOPCs from hiPSCs

Another parameter for successful cell therapy is the choice of cell type and state of differentiation. We derived hOPCs from hiPSCs using FGF3/FGF10 induction in a monolayer culture system (Figure 3A) as previously reported.^{25,29} The differentiation of hOPCs was monitored by analyzing the expression of a subset of gene markers for otic progenitor lineage^{10,37} by qPCR and immunocytochemical analyzes. Cell cultures were treated with FGF3/FGF10 for 13 days showed a significant upregulation in the relative expression levels of transcripts of otic progenitor markers (*gata3*, *dlx5*, *bmp4*, and *pax2*) as compared to undifferentiated hiPSCs at day 0 (Figure 3B). The expression of some of these otic lineage markers was further confirmed by immunohistochemistry (Figures 3C–3H). To evaluate the *in vitro* differentiation potential of hiPSC-derived early otic placodal

pooled data ($n \geq 3$ per group) are represented by the means (dot) \pm SD (error bar). Wilcoxon rank-sum test, no statistically significant differences were found between groups before and after cochleostomy. RW, round window; ST, scala tympani. Scale bars, 500 μ m.

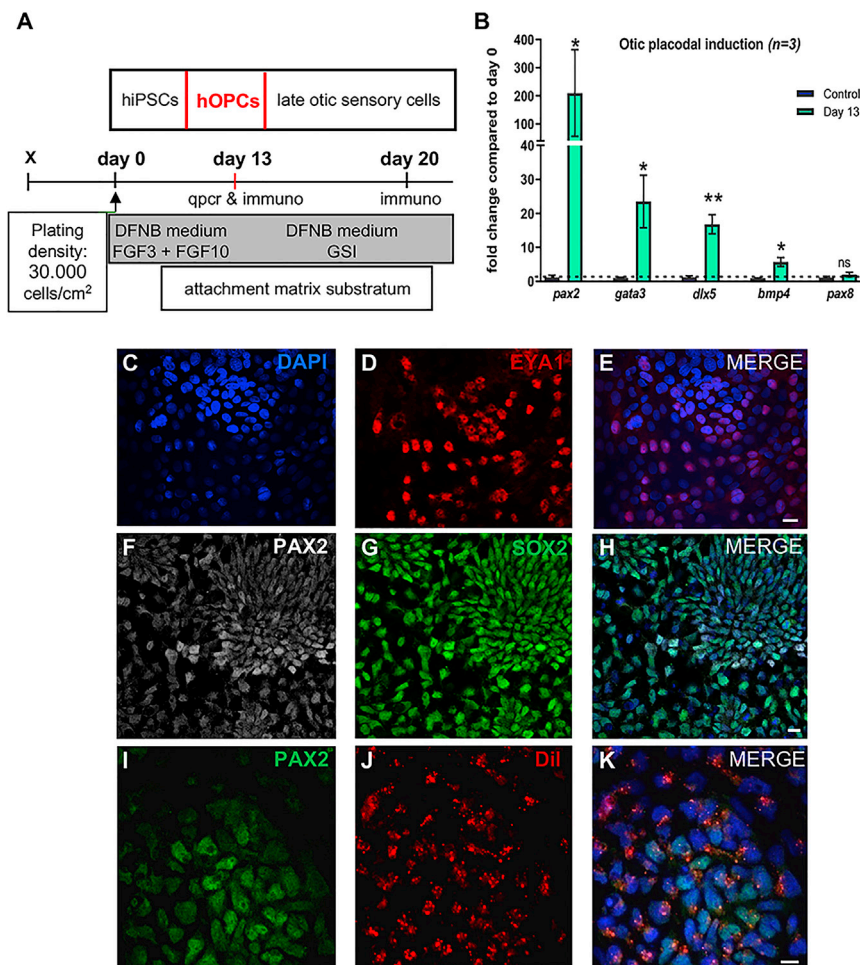


Figure 3. Schematic Illustration of the Generation of Human Otic Progenitors from iPSCs Using a Monolayer Culture Protocol

(A) Schematic representation of otic progenitor cells generation from hiPSCs by exposure to FGF3 and FGF10 (50 ng/mL each) in DFNB medium for 13 days *in vitro*. In some FGF-treated cultures, hOPCs at day 13 *in vitro* were differentiated into late otic sensory cells by exposure to GSI (5 μM) until day 20. (B) QPCR analysis of a panel of known otic progenitor (*pax2*, *gata3*, *dlx5*, *bmp4*, *pax8*) gene markers in FGF-treated cultures at day 13 as compared to their relative expression levels in undifferentiated hiPSCs at day 0. Relative gene expression levels were normalized against *gapdh* gene and compared to hiPSCs at day 0. Group means and SD are shown. An unpaired Wilcoxon matched-pairs signed-rank test was used for single comparisons; statistical differences are indicated by **p* < 0.05, ***p* < 0.01; ns, no statistically significant difference (*n* = 3). (C–H) Representative immunostainings for EYA1 (D) PAX2 (F), and SOX2 (G) in day 13 FGF-treated cultures. A population of PAX2 (shown in white), SOX2 (shown in red), and EYA1 (shown in red) immunopositive cells are observed in these differentiated cultures. DAPI staining is shown in blue. (I–K) A sample of differentiated cells at day 13 was labeled with the Vybrant-Dil (J) tracer and immunostained with PAX2 antibody (I). Double labeling (K) indicated that virtually all Dil-labeled cells (shown in red) are immunopositive for PAX2 (shown in green). DAPI staining is shown in blue. FGF, fibroblast growth factor; DFNB, DMEM/F12 with N2/B27; GSI, gamma secretase inhibitor. Scale bars, 20 μm in all panels.

progenitors obtained at day 13, some FGF-treated cultures were kept for one additional week in culture medium with gamma-secretase inhibitor.²⁹ Immunostaining analysis of cultures at day 20 revealed a subset of differentiated cells co-expressing MYO7A and POU4F3 markers (Figure S2).

Prior to cell transplantation, the hOPCs generated at day 13 *in vitro* were stained with Vybrant-Dil tracer. This fluorescent dye has been previously used to study trafficking of implanted mesenchymal stem cells into the heart muscle,³⁸ human olfactory stem cells in the mouse cochlea,²¹ and mesenchymal stem cells in inflamed ear.³⁹ In an initial characterization step before engraftment, we observed that virtually all PAX2-immunopositive hOPCs were labeled with the Vybrant-Dil (Figures 3I–3K). We then assessed the distribution, integration, and differentiation of these Dil-labeled hOPCs when implanted in the drug-damaged adult guinea pig *in vivo*.

Human Otic Progenitor Transplantation Triggered an Immune Response in Ototoxic-Exposed Cochleae

The Dil-labeled cells were injected into the cochleae of ototoxic-treated guinea pigs by cochleostomy at the basal turn (Figures 2B–2D). It is

well known that microglia-macrophages (IBA1-positive cells) are up-regulated in response to local cochlear damage induced by ototoxicity or noise exposure.^{40,41} For this reason, we analyzed the presence of IBA1-immunopositive cells in ototoxin-damaged animals after engraftment (Figures 4B–4G). We found that in amikacin-ungrafted control cochlea, a subset of IBA1-immunopositive cells were principally located at the modiolus (Figure 4E). In contrast, in amikacin-treated post-grafted cochlea, we observed IBA1-expressing cells increased at the modiolus (Figure 4G), but they were also localized at the vicinity of injected Dil-labeled cells in other areas, i.e., the basal part of the organs of Corti (Figures 4C and 4D). In addition, double labeling revealed that some Dil cells were immunopositive for IBA1 (Figures 4C and 4D), suggesting possible initiation of an immune response following injection of hOPCs into amikacin-treated cochleae. We have also observed a moderate IBA1 immunoreactivity in some damaged HCs mostly those of amikacin-treated day 4 post-grafted cochlea (Figure 4C).

Previous data in guinea pigs have reported macrophages in the area of degenerating cells, in the tunnel of Corti, and OHC region.⁴² More recently, active macrophages were seen in the organ of Corti area

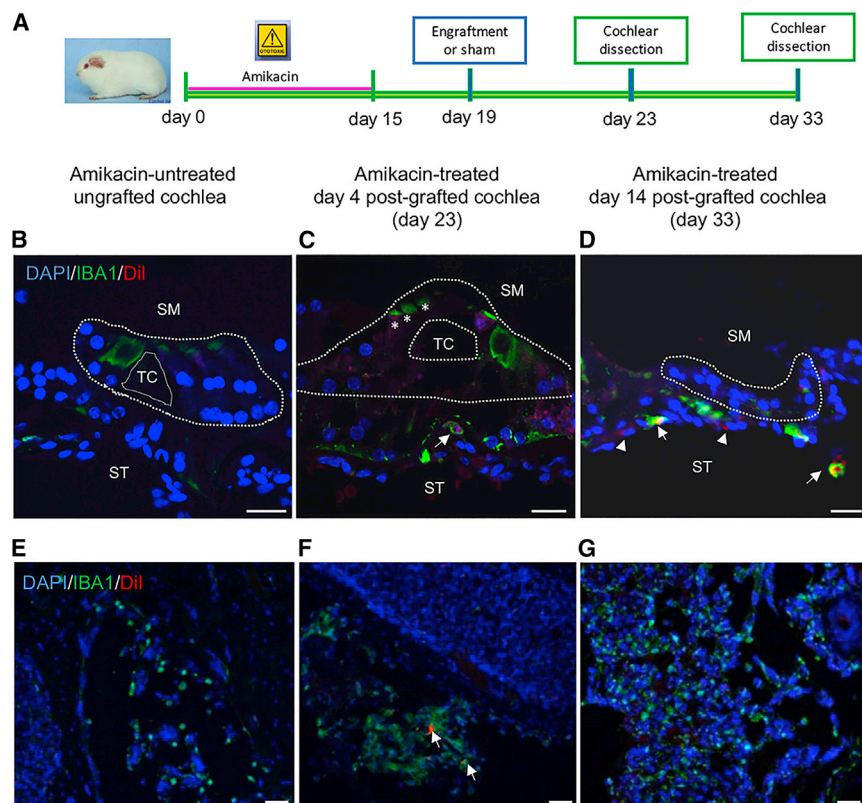


Figure 4. Human Otic Progenitors Trigger an Immune Reaction after Transplantation

(A) Timeline of experimental design for hOPC transplantation into control and implanted drug-exposed cochleae. (B–D) IBA1-immunopositive cells (shown in green) are revealed by immunohistochemistry on transverse sections from cochleae of control untreated (B), no-implanted, 4 days post-implanted (C), and 14 days post-implanted drug-treated animals (D). The Vybrant-Dil-labeled cells are shown in red. Some of IBA1-immunopositive cells are observed at the basal part of the damaged organs of Corti (arrows). A slight IBA1 immunoreactivity was detected in some hair cells mostly those of amikacin-treated day 4 post-grafted cochlea (C, asterisks). Arrowheads show Dil-positive/IBA1 negative cells in (D). (E–G) Representative images from the modiolus areas of amikacin-untreated ungrafted animals (E) and amikacin-treated day 33 post-grafted animals (G) showing expression of IBA1 in many cells. (F) In the modiolus of amikacin-treated day 4 post-grafted animals, few Dil-labeled cells (shown in red, arrows) were surrounded by IBA1 immunostaining (shown in green, arrows). Nuclei were revealed by DAPI staining (shown in blue). Scale bars, 20 μ m in all panels. SM, scala media; ST, scala tympani; TC, tunnel of Corti.

near damaged auditory HCs in the adult human inner ear.⁴³ Furthermore, active IBA-immunopositive cells were also found to be closely associated with the OHCs in the human inner ear.⁴⁴ Whether macrophages are derived from activated resident cells or represent externally recruited cells remains unknown.

Distribution of hOPCs in Ototoxic-Damaged Cochleae

To analyze the spatial distribution of implanted hOPCs in ototoxic-damaged cochleae, we used whole-mount surface preparations and tissue clarification methods (Figures 5A–5G). The cochlear clearing procedure was shown to preserve the complex 3D structure of the cochlea at the same time reducing tissue distortion.⁴⁵ This methodology was applied to analyze the distribution of grafted cells at different turns of the cochlea. Interestingly by combining tissue clarification technique and confocal microscopy, we were able to visualize a widespread distribution of Dil-labeled cells in different turns of damaged-cochleae 14 days post-cell-implantation (Figures 5A–5D; Video S1). Using greater magnifications at the level of a given cochlear turn along the basal-to-apical longitudinal axis allowed to visualize the Dil-labeled cells within the amikacin-damaged cochlear sensory epithelium (Figures 5C and 5D). Furthermore, whole-mount surface preparations from micro-dissected damaged cochleae allowed cell imaging through the depth of the cochlear sensory epithelium in areas corresponding to frequencies from 8 to 16 kHz (Figure 5E). We observed Dil-labeled cells intercalating within the layers of the cochlear sensory epithelium. In addition, the projections of all

Z stacks obtained by confocal microscopy allowed for virtual transverse views of the cochlear sensory epithelium. A representative image of a multiplanar 3D reconstruction allowed us to recognize the general architecture of the organ of Corti and to visualize some fluorescent cells positioned at the level of nuclei from surrounding epithelial cells (Figure 5F).

In order to better describe the position of Dil-positive cells, HCs were revealed by immunohistochemistry against MYO7A. We observed some Dil-positive cells within the cochlear sensory epithelium at the level of HC area (Figure 5G). The presence of Dil-hOPCs in different cell layers is suggestive of a potential incorporation within the cochlear sensory epithelium 14 days post-implantation.

Number of hOPCs and Their Migration Increased in Cyclosporin-Pre-treated Animals

There exists compelling evidence showing the favorable effect of immunosuppression on grafting cells into the cochlea.^{25,32} To ameliorate the conditions of hOPC injection, we used immunosuppression in ototoxic-damaged cochleae by administration of cyclosporin (Figure 6A). An initial qualitative analysis of Dil-labeled cells in cochlea whole-mount preparations showed that in cyclosporin-treated animals, the Dil-signal was often surrounding the nuclei of the cochlear sensory epithelium while the Dil signal displayed a punctate pattern along the cochlear epithelium in cyclosporin-untreated animals (Figure 6B). We then quantified the number of Dil-labeled cells in the cochlear sensory epithelium at different turns. In cyclosporin-treated animal, the distribution of fluorescent cells showed a gradient from

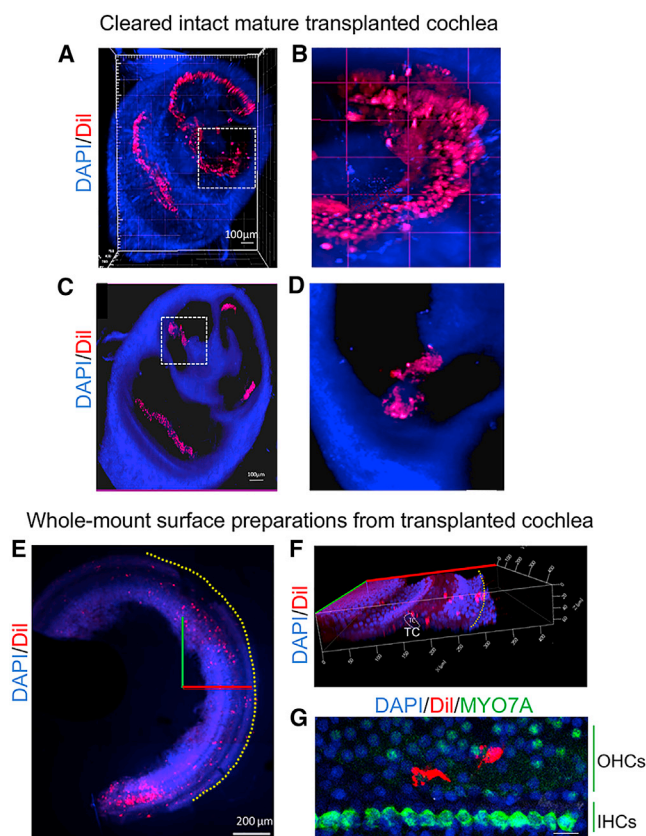


Figure 5. Stereological Imaging of Fluorescent Dil-Labeled Otic Progenitors in Ototoxic Damaged Cochlea

(A–D) The distribution of Dil-labeled cells was analyzed on grafted cleared mature guinea pig cochlea imaged through its entire volume. (A) Representative 3D reconstruction obtained from cochlea dissected at 14 days post-implantation after tissue clearing. Dil-labeled cells (shown in red) were observed at different cochlear turns. (B) Magnification of dotted area in (A) allowed to visualize Dil-labeled cells (in red) within the cochlear epithelium. (C) Virtual transversal slice obtained from (A), where it is possible to observe some Dil-labeled cells at level of organ of Corti region. (D) Magnification of dotted area in (C) showing the organ of Corti region. (E) Distribution of Dil-labeled cells was analyzed on cochlear whole-mount surface preparations. The X (in red) and Y (in green) axes are represented in the image. Yellow dotted line indicates the area of the stria vascularis. (F) Virtual 3D reconstruction of the cochlear sensory epithelium was obtained by transposition of Z-stack images acquired from whole-mount preparations with confocal microscopy. The X (red line), Y (green line), and Z (blue line) axes are represented in the image. (G) MYO7A-immunopositive cells (shown in green) were revealed at the level of IHCs row by immunohistochemistry. Some Dil-positive cells were also observed in the OHC region. Nuclei were revealed by DAPI staining (shown in blue). Scale bars, 100 μ m (B and C), 200 μ m (E), and 20 μ m (G). TC, tunnel of Corti; IHCs, inner hair cells; OHCs, outer hair cells.

base-to-apex with a significant number of Dil-labeled cells found at the basal and second cochlear turns (Figure 6C).

These observations suggest that grafted cells are localized preferentially within damaged regions of cyclosporin-pre-treated animals. Furthermore, we determined the position of Dil-labeled cells within

the cochlear sensory epithelium by using a compilation of Z stacks and an image processor. This analysis allowed the generation of optical transverse slides from the 3D images that clearly showed the cochlear sensory epithelium from the basilar membrane to the reticular lamina (Figure 6D). In these transverse images, we measured the distance of Dil-labeled cells from the basilar membrane to the reticular lamina. In cyclosporin-treated animals, Dil-labeled cells were preferentially observed (62.2%) at 10–20 μ m distance from basilar membrane, and a significant number of cells (15.1%) were observed beyond 20 μ m from basilar membrane. In contrast, in cyclosporin-untreated animals Dil-labeled cells were mostly observed (67%) at 0–10 μ m and only 3.9% beyond 20 μ m distance between the basilar membrane and reticular lamina (Figure 6E).

For easy tracking of distribution of Dil-labeled cells, we referred to the cochlear sensory epithelium a region that contains one row of inner HCs and three rows of outer HCs separated by supporting cells that connect the reticular lamina and basilar membrane (Figures 6B–6E).

Human Otic Progenitors Can Differentiate *In Vivo* into Cells Expressing Late Otic Sensory Markers

After *in vitro* characterization of hOPCs and their ability to migrate and integrate within different areas of the *in vivo* cochlea, we explored their cell fate 2 weeks after transplantation. The profile of late otic sensory marker expression of Dil-labeled cells was analyzed in drug-damaged cochleae by immunohistochemistry (Figure 7A). In a transverse section of the organ of Corti, a subset of Dil-labeled cells was found below the supporting cell area. In this area, we detected patches of Dil-labeled hOPCs that were moderately immunopositive for MYO7A, suggesting their initial differentiation into cells expressing initial HC markers (Figures 7B and 7B'). These MYO7A-immunopositive cells are clearly distinguished from residual remaining HCs located at the apical part of the organ of Corti (Figure 7A). The Dil-labeled cells in the spiral ganglion area were not immunopositive for otic sensory markers (Figure 7A). Also, in a projection of a confocal image of whole-mount surface preparation, we found few Dil/MYO7A-positive cells in the cochlear sensory epithelium (Figures 7C and 7D'). Furthermore, at the basal area of the organ of Corti, we observed some engrafted Dil-labeled cells that were also immunopositive for SOX2 (Figures 7E and 7F'). The presence of Dil-labeled cells that expressed the SOX2 may suggest that some hOPCs are also able to differentiate into supporting cells. Our results indicate that some transplanted hOPCs can migrate and incorporate into the basal part of organ of Corti and initiate differentiation into cells expressing sensory markers, i.e., MYO7A and SOX2.

Grafted Mouse GFP-HC Progenitors Are Able to Migrate and Integrate Sensory Epithelium of Ototoxin-Damaged Cochleae

In order to corroborate the results obtained with hOPCs, we used the same injection approach for implantation of HC progenitors derived from *Atoh1*-GFP reporter mice as donor cells. We have previously demonstrated that otic progenitors derived from mouse embryonic stem cells of *Atoh1*-GFP reporter mice are able to integrate and

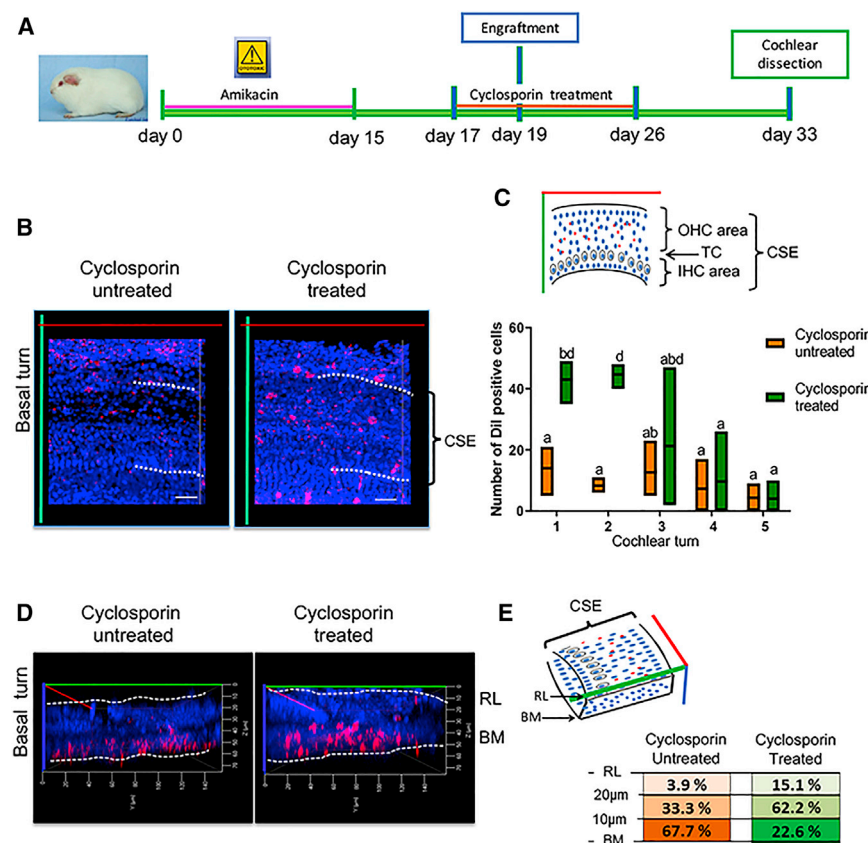


Figure 6. Number of Surviving Transplanted Cells Increased in Animals Pre-treated with Cyclosporin

(A) Timeline of experimental setup for hOPC transplantation in cyclosporin-treated versus cyclosporin-untreated grafted animals. (B) Representative images of the whole-mount surface preparation of cochlear epithelia at 14 days post-implantation. Dil-labeled cells (red) correspond to grafted hOPCs and nuclei were stained with DAPI (blue). (C) The number of Dil-labeled cells were quantified in cochlear sensory epithelium area at different cochlear turns. The CSE was represented in the space between dotted line in (B). Cyclosporin-treated group is represented in green color, and cyclosporin-untreated group is represented in orange color. Each floating bar represents group means (line) and min to max (box) values ($n = 3$). ANOVA test was used for multiple comparisons; different letters indicate significant differences between groups (** $p < 0.005$). (D) Virtual transversal images of cochlear sensory epithelium were obtained by 3D reconstructions of Z-stack series. Schematic reference to basilar membrane (BM) and reticular lamina (RL) is shown with dotted lines. The distance of Dil-labeled cells from basilar membrane was determined by Zen software. (E) The percentages of cells found at different distances was determined by the ratio of number of cells quantified in a delimited distance/total number of cells quantified into the entire turn of the cochlea. Data shown correspond to the basal turn of the cochlea from cyclosporin-treated (shown in green) and cyclosporin-untreated (shown in orange) animals. CSE, cochlear sensory epithelium; OHC, outer hair cell; IHC, inner hair cell; BM, basilar membrane; RL, reticular lamina. Scale bar, 20 μ m.

differentiate in organotypic cultures of ototoxin-damaged mouse cochleae.⁴⁶ In this study, we implanted HC progenitors derived from *Atoh1*-GFP reporter mice as described previously⁴⁷ in the guinea pig model of ototoxicity. Grafted cochleae were analyzed 4 weeks post-transplantation in whole-mount surface preparations (Figure 8A). Some *Atoh1*-GFP cells were found in the cochlear sensory epithelium (Figure 8B), suggesting their ability to migrate and survive within *in vivo*-damaged cochleae. Furthermore, some mouse *Atoh1*-GFP cells were observed close to the supporting cell area, and they were immunopositive for POU4F3. We found a few POU4F3/*Atoh1*-GFP cells located just below endogenous inner HCs that were immunopositive for HC markers MYO7A/POU4F3 (Figures 8B–8E). Multiplanar reconstruction by confocal imaging confirmed that few grafted *Atoh1*-GFP cells were positioned in the supporting cell area below the inner HC layer (Figures 8D and 8E). These engrafted cells were likely undergoing initial stages of differentiation into HCs. Thus, the results obtained from these *in vivo* cell transplantation experiments demonstrate that transplanted otic progenitors can survive and migrate to the cochlear sensory epithelium and that some of them initiate differentiation into cells that express otic sensory markers.

DISCUSSION

As the regeneration capacity of the sensory epithelium is limited, a stem cell therapy approach for the inner ear is a promising therapeutic

strategy to treat sensori-neural hearing loss. The goal of our study was to derive characterized donor hOPCs *in vitro* and to determine if they could migrate and differentiate after engraftment into a clinically relevant mammalian model of partial hearing loss.

The most suitable donor cells for cell transplantation *in vivo* for the treatment of sensorineural hearing loss may differ, depending on the origin of the injury and the cell type lost. When considering cell therapy for hearing loss, the most suitable donor cells for transplantation may ideally be progenitor cells destined to become HCs. The level of differentiation of the donor cells may also affect the subsequent rate of engraftment of cells into target organs. Previous cell transplantation experiments suggest that cells grafted at lower levels of differentiation generally have a risk of tumor formation, and cells grafted at moderate levels of differentiation have higher engraftment rates into the target sites, although with a lower survival rate.^{18,48}

Human otic progenitors are partially differentiated epithelial progenitors that express *PAX2*, *GATA3*, and *DLX5* and can be further differentiated *in vitro* into cells expressing initial HC markers (Figure S2). Because of the expected advantage in survival and engraftment rates, we chose hiPSC-derived hOPCs at day 13 *in vitro* for implantation *in vivo*.

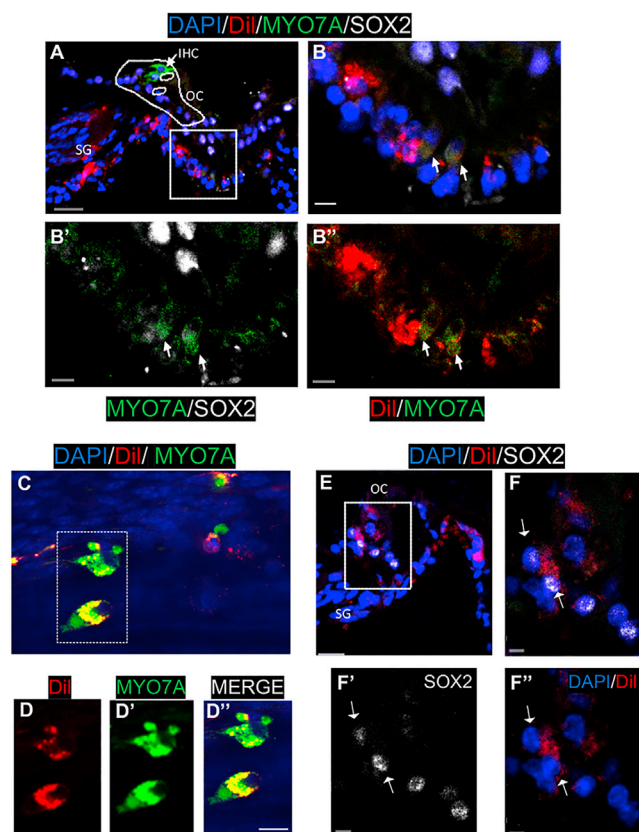


Figure 7. Human Otic Progenitors Expressed Late Otic Sensory Markers 14 Days Post-implantation In Vivo

(A) Transplanted Dil-hOPCs in a transverse section of drug-treated cochlea. A projection of a confocal image stack showing MYO7A (shown in green) and SOX2 (shown in white) immunoreactivity, Vybrant-Dil (shown in red), and nuclear DAPI staining (shown in blue). We observed a complete loss of OHCs, but the IHC (arrow) remained in the ototoxin-damaged organ of Corti (OC, dotted line). (B–B'') Enlarged region of boxed area in (A) showing MYO7A/Dil-positive cells (arrows) at the basal part of the organ of Corti. (C) Area from whole-mount surface preparation of another ototoxin-damaged and grafted cochlea showing two Dil-labeled cells (red) immunopositive for MYO7A (green). (D–D'') Magnification of a dotted area in (C) with separated channel combinations: Dil-labeled cells (red), MYO7A-immunopositive cells (green), merge (yellow). (E) A confocal image of another ototoxin-damaged cochlea showing implanted Dil-labeled cells and nuclear SOX2 immunostaining (white). (F–F'') A magnification of boxed area in (E) revealed some SOX2/Dil cells at the basal area of the organ of Corti (arrows). Scale bars, 20 μ m (A and E), 10 μ m (C and F), and 5 μ m (B'–B'', D'–D'', and F'–F'').

We observed that some of the Dil-labeled hOPCs survived *in vivo* for at least 2 weeks after transplantation and migrated throughout every cochlear turn. The Dil-labeled cells engrafted principally in non-sensory regions, i.e., stria vascularis and spiral ligament (data not shown), and a subset of injected cells was found in the scala media compartment near the organ of Corti. The widespread distribution of hOPCs *in vivo* and their survival throughout the cochlea were indicative of effective delivery of donor cells at a moderate stage of differentiation and the timing of cell injection. Four days post-ototoxic exposure was chosen for the injection time, because preliminary ex-

periments indicated that the number of engrafted cells decreased as the interval between damage and onset of transplantation increased.⁴⁹ However, future studies should systematically investigate different times after ototoxic exposure for injection of hOPCs. It seems likely that the primary mechanism behind the widespread intra-cochlear distribution of injected cells occurs through the perilymphatic space via the movement of perilymph, which flows at a slow 1.6 nL/min in an apical direction.⁵⁰ The post-auricular surgical approach used in our experiments was minimally invasive to the cochlea, as the ABR threshold shifts in all the frequency response regions tested were similar before and after cochleostomy. Nonetheless, a moderate and limited inflammatory response was observed after the injection of hOPCs. This reaction was revealed by the expression of IBA1, which is a marker of macrophages/microglia.⁵¹ IBA1-immunopositive cells appeared at day 4 post-transplantation in ototoxic-grafted cochlea, suggesting that the behavior of injected hOPCs could be affected by endogenous tissue reactions. Previous studies suggested cell survival *in vivo* did not incite an immune reaction, because the cochlea is a relatively immunoprivileged site,⁹ but it is not clear what criteria were used to assess immune responses. In addition, several studies reported the presence of resident tissue macrophages in the inner ear, particularly in the spiral ligament, spiral ganglion, and the basilar membrane area.⁵² There is also evidence that cochlear macrophages can be recruited from blood-borne monocytes to damaged and dying HCs induced by noise and ototoxic drugs^{41,53,54} and can induce inner ear inflammation.^{55,56}

In order to reduce the inflammatory response, whatever its origin, we used a daily intramuscular injection of cyclosporin starting 2 days before and continuing for 7 days after the injection of hOPCs in our delivery assay. Interestingly, we found that significantly more hOPCs had migrated beyond the basilar membrane area toward the scala media in grafted animals pretreated with cyclosporin as compared to the untreated controls. The hOPCs engrafted along different cell layers within the sensory epithelium from the basilar membrane to the reticular lamina, which marks a division between the endolymphatic and perilymphatic compartments.

These observations demonstrate the value of transient and moderate immunosuppression in enhancing the number of migrated hOPCs within the sensory epithelia of ototoxin-treated cochlea. By using scanning confocal imaging of intact cleared cochlea, we were able to reconstruct a 3D image of a damaged cochlea 14 days post-transplantation, when we observed a considerable number of engrafted cells in damaged cochlear sensory epithelium. The projection images at different Z stacks allowed us to visualize Dil-labeled cells that integrated within the cochlear sensory epithelium, including the organ of Corti. Although the proportion of donor cells in the scala media was modest via this delivery approach, it would suggest that hOPCs migrated into the endolymphatic compartment from the perilymphatic region. At present, we can only speculate as to the mechanism by which these cells reach the cochlear sensory epithelium. It is possible that some minor, transient damage to the basilar membrane created

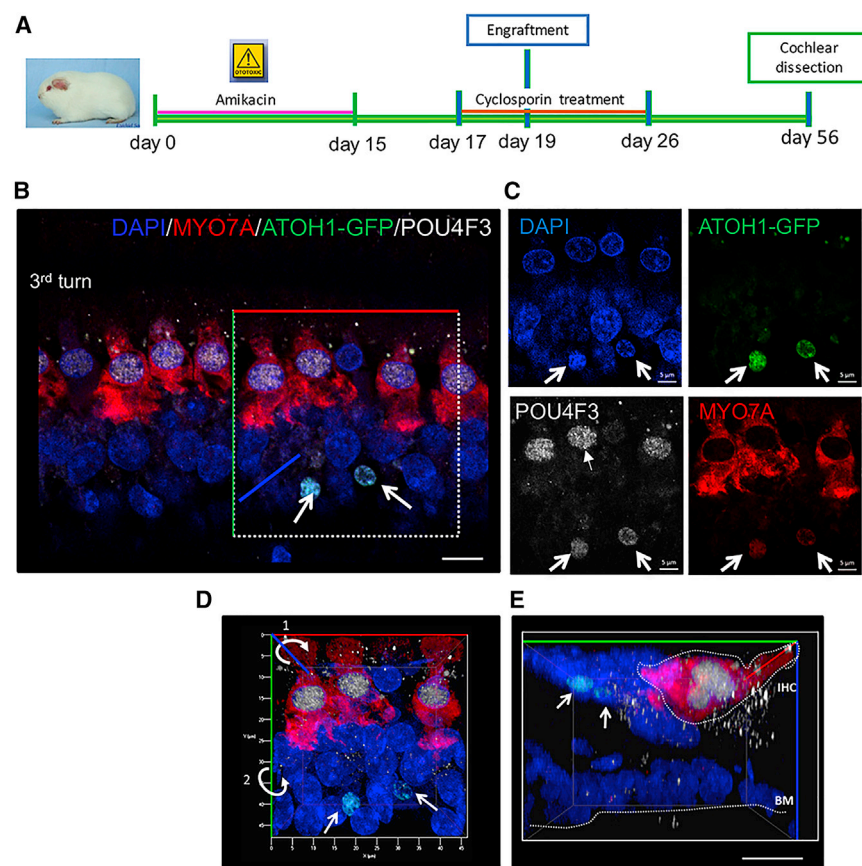


Figure 8. Survival, Distribution, and Cell Fate of Mouse *Atoh1*-GFP Progenitor Cells 4 Weeks Post-transplantation

(A) Timeline of the experimental design used for *Atoh1*-GFP progenitor cell transplantation including cyclosporin treatment. (B) The HC markers MYO7A (shown in red) and POU4F3 (shown in white) were observed on cochlear whole-mount surface preparations as revealed by immunohistochemistry. Few *Atoh1*-GFP-injected cells (shown in green) migrated to the cochlear sensory epithelium and were found below the IHC region (MYO7A/POU4F3) immunopositive cells. (C) Engrafted *Atoh1*-GFP cells (green) moderately expressed the POU4F3 (shown in white, arrows). (D) 3D reconstitution of whole-mount preparation outlining the X (in red), Y (in green), and Z (in blue) axes. (E) Virtual transverse image confirming the spatial localization of *Atoh1*-GFP engrafted cells (arrows) in the area below the MYO7A immunopositive endogenous residual IHC. Scale bar, 10 μ m (B and E) and 5 μ m (C). IHC, inner hair cell; BM, basilar membrane.

an appropriate route for migration of injected progenitors from scala tympani to scala vestibuli.

To our knowledge, this is the first study to report transplanted exogenous human progenitors that were able to integrate at different levels along the width of the cochlear sensory epithelium of ototoxin-treated animals. The integration of hOPCs into the cochlear sensory epithelium may be especially important for their long-term survival and further differentiation.

In order for hOPCs and cell-injection assays to be of clinical relevance, implanted cells must differentiate into sensory cells or other cell types, based on the inner ear disease being treated. Numerous studies have described protocols for differentiating stem cells into human HC-like cells under different *in vitro* conditions.^{27–29} The ability to manipulate cells once they are transplanted into living damaged cochleae is limited and is a challenging area for sensory regeneration.

Most transplantation studies have been directed at replacing degenerating auditory neurons, and several cell types have been delivered into the mammalian cochlea, including embryonic stem cells,^{32,34} bone marrow stem cells,^{57–59} neural stem cells,^{21,60,61} and neural otic progenitors.^{24,25} In contrast, only a small number of studies have explored targeting cells to the cochlear sensory epithelium,^{18–20,33}

and none have provided evidence of the differentiation of transplanted cells into sensory cells.

In our studies, we attempted to determine the phenotype of hOPCs that incorporated into damaged cochlear sensory epithelium. The transplanted Dil-labeled hOPCs survived for at least 2 weeks and integrated into the organ of Corti of ototoxic deafened guinea pigs.

Similar integration at the level of the organ of Corti has been reported, with neural stem cells injected into sound-damaged guinea pig.²¹ We observed a subset of Dil-labeled transplanted cells moderately immunopositive for initial HC (MYO7A and POU4F3) markers. The hOPCs found outside the area of the organ of Corti (i.e., modiolus) were not immunopositive for MYO7A. This observation suggests that the host microenvironment within the organ of Corti may provide specific cues to promote differentiation toward an epithelial phenotype. Host microenvironment has been observed to play a role in instructing the behavior of transplanted cells for neural stem cells^{59,60} and stem cells transplanted into mice with noise-induced hearing loss.⁶¹ A recent study used self-assembling amphiphilic peptide molecules to create a niche that supported neuronal differentiation and survival *in vitro* and *in vivo* after transplantation into rodent inner ears.²² We also confirmed the migration and survival of transplanted progenitors in the organ of Corti using an *Atoh1*-GFP mouse reporter cell line.

At 4 weeks post-grafting, mouse *Atoh1*-GFP cells were visualized in the organ of Corti by their endogenous fluorescence and had initiated differentiation into cells expressing HC markers.

Our results suggest that the mature mammalian cochlea retains the signals necessary to influence stem/progenitor cell differentiation

along a sensory phenotype, even though it cannot regenerate these cells from its endogenous cell population.

This is the first report of the successful delivery of partially differentiated hOPCs into an animal model of sensorineural hearing loss. Furthermore, we observed that transplanted hOPCs could migrate and survive in *in vivo* damaged mature cochlea for at least 2 weeks after implantation, and some cells integrated into the basal area of the organ of Corti and moderately differentiated into cells with phenotypic characteristics of initial hair and supporting cells. Future experiments will need to determine how to induce specific interactions between the transplanted cells and the endogenous cochlear tissue to allow differentiation of the engrafted cells and allow recovery of cochlear function.

MATERIALS AND METHODS

Animal Model of Ototoxic Drug-Induced HC Death and Hearing Loss

All experimental procedures were conducted on adult guinea pigs (Dunkin Hartley breed from Charles River Laboratories) in accordance with national and European Union regulations (EU directive N2010/63) and in agreement with the authorization for animal experimentation attributed to the laboratory by the “Prefecture des Bouches du Rhône” (permit number B1305525). All efforts were made to minimize animal suffering and to reduce the number of guinea pigs used in this study. Auditory hearing loss was induced by the administration of amikacin (Sigma) at the doses of 400 mg/kg/day during 15 days via intramuscular injection. Auditory threshold loss was analyzed by ABR by comparing the auditory threshold of animals before and after treatment.

Animal Immunosuppression

Guinea pigs with and without immunosuppression were used for otic progenitor injection into the cochleae. A group of animals received cyclosporin (Novartis) by oral administration at the doses of 15 mg/kg body weight dissolved in sunflower oil. A control group received only the vehicle. The cyclosporin administration started 2 days before surgery and pursued until 7 days post-grafting.

In Vitro Differentiation of hOPCs

Induced pluripotent stem cells (ChiPSC-4; RRID:CVCL_RM97) were derived from healthy donor human dermal fibroblasts (Cellartis by Takara Bio Europe) using retrovirus technology based on the transduction of the transcription factors Oct3/4, Sox2, Klf4, and c-Myc.²⁶ The hiPSCs were plated at a density of 40,000–50,000/cm², and when the cells were confluent at 90%, they were passaged using TrypLE (Life Technologies). The otic induction was performed using the methodology reported in previous studies.^{23,27} In brief, the hiPSCs were cultured in DFNB (DMEM/F12 with N2 and B27 serum-free supplements) medium with FGF3 and FGF10 (50 ng/mL each) from the first day (day 0) until the end of the differentiation period at day 13 or day 20 in the presence of gamma secretase inhibitor at 5 μ M, i.e., difluorobenzeneacetamid (DBZ; Tocris Bioscience). qPCR

and immunostaining were performed on differentiated cells and analyzed for the expression of otic progenitor markers.

Generation of Otic Progenitors from Atoh1-GFP Mice

Atoh1-nGFP mice were used to generate otic progenitors as previously described.⁴⁷ In brief, the cochleae of neonatal mice were dissected, and the organ of Corti was separated from the stria vascularis and the modiolus. The organs of Corti were then treated with Cell Recovery Solution (Corning) to discard the underlying mesenchyme. Epithelia were then collected and treated with TrypLE (Life Technologies) to obtain a single cell suspension. Cells were centrifuged and resuspended in Matrigel for cell culture. Cells were cultured and were induced to differentiation into otic cell lineage as described previously.⁴⁷

Human Otic Progenitors Staining before Cell Injection

Otic progenitors at day 13 were labeled with the lipophilic dye Vybrant-Dil cell-labeling solution (Molecular Probes). Otic progenitors were incubated in Dil-labeling solution (1:200) during 20 min at 37°C. The cells were washed in DMEM medium and dissociated using TrypLE. For transplantation, cells were re-suspended in DMEM at the density of 1×10^4 cells per μ L. A total volume of 4 μ L was injected into the cochleae.

Microsurgery for Human Otic Cell Injection into Adult Cochleae

The surgical protocol used here was adapted from Hildebrand et al.¹⁸ Cochleostomy was performed under anesthesia by intramuscular injection of ketamine (40 mg/kg body weight, Virbac France laboratories) and xylazine (8 mg/kg body weight, Bayer Laboratories) 5 days after ototoxic trauma. A surgical setup was adapted from a stereotaxic instrument to ensure the maintenance of Hamilton syringe and forceps to immobilize the guinea pig head. A post-auricular approach was used to expose the tympanic bulla, which was opened with a surgical drill of about 4 mm diameter. Cochleostomy was performed under stereomicroscopy to visualize the cochlea. Soft surgery techniques were used to perform a cochleostomy with a 0.1-mm diameter drill in the lateral wall of scala tympani at the basal turn, maintaining an intact bony rim of about 1 mm from the round window. Then, 4 μ L of culture medium containing around 1×10^4 human otic progenitors were infused into the scala tympani. At the end of the procedure, the holes in the cochlea and tympanic bulla were sealed with muscle and the wound sutured (3-0 bis mersilk suture, Ethicon).

ABR Threshold Determination

ABRs were recorded by scalp needle electrodes underneath the skin at the vertex (active electrode), behind mastoid of the tested ear (reference electrode), and in neck muscle (ground electrode). For stimulus generation and presentation, data acquisition, and offline analysis, we used a custom-written MATLAB software (The MathWorks) coupled to a SoundMax Integrated HD audio chip. Signals were amplified through a TDT SA1 amplifier and fed to Sennheiser C870 earphones coupled to the animal ear via a 1 cm silastic tube glued at the entrance of the external acoustic meatus. Tone pips of 2 ms linear rise and fall times and no plateau were used at octave frequencies between 2 and

32 kHz. Sounds were presented at a rhythm of 20 per s at from 90 to 0 dB sound pressure level (SPL) in 10-dB steps. The ABR responses were amplified using A-M systems 17000 amplifiers with a gain of 10,000 and filtered between 100 and 5,000 Hz. Signals were fed to a CED 1401 digital converter and averaged over several hundred sweeps. The hearing thresholds were determined by visual inspection as the lowest stimulus intensity that evoked a reproducible response waveform in the recorded averages.

qRT-PCR

Total RNA was extracted from undifferentiated and differentiated cells using the PureLink RNA mini-kit (Life Technologies) according to manufacturer's instructions. cDNA was synthesized from 1 µg of RNA (per sample) using a high-capacity RNA-to-cDNA kit (Life Technologies); 5 µL of cDNA were submitted to qPCR reaction. The qPCR was performed with TaqMan fast real time PCR system, according to the manufacturer's recommendations (Applied Biosystems). Primer pairs used were listed in supplemental data (Table S1). Gapdh gene served as an endogenous control. For each experiment, different cDNA samples were analyzed in duplicate. Relative gene expression values were determined using the comparative $2^{-\Delta\Delta Ct}$ method after normalization to Gapdh gene.

Tissue Processing and Immunohistochemistry

Animals were perfused with 4% paraformaldehyde (PFA) in 0.1 M PBS. The cochleae were dissected and post-fixed overnight after opening the round and oval windows. They were then decalcified in 10% EDTA and 1% PFA solution at room temperature (RT) for 2 weeks. For transverse sections with a cryotome, cochleae were transferred to 30% sucrose at 4°C overnight and embedded in OCT. Serial sections (16 µm) were mounted on Ultra-StickGold Seal glass slides (Becton Dickson) and stored at -80°C. For whole-mount surface preparations, the cochlear sensory epithelium was dissected out from decalcified cochleae. Each cochlear basal turn was micro-dissected for further analysis.

Specimens were fixed at RT in 4% PFA for 20 min followed by permeabilization with 0.5% Triton X-100 and incubated with primary antibodies overnight at 4°C. Secondary antibodies (Alexa Fluor 488, Alexa Fluor 568, and Alexa Fluor 647 conjugated; Invitrogen) were used at 1:500 dilution. Nuclei were visualized with DAPI (Vector Laboratories). Primary antibodies used were as follows: rabbit anti-PAX2 (Eurogentec, 1:200), mouse anti-MYO7A (DSHB, 1:200), rabbit anti-MYO7A (Proteus, 1:200), goat anti-SOX2 (Santa Cruz, 1:200), rabbit anti-IBA1 (Wako, 1:200), and mouse anti-POU4F3 (Abnova, 1:200). Primary antibodies are listed in Table S2.

Cochlea Clearing and Imaging

Inner ears were collected from adult guinea pigs. Animals were perfused under deep anesthesia with 4% PFA in PBS containing 0.9% sodium chloride buffer (pH 7.4). Each temporal bone was dissected to expose the cochlea, the stapes removed, and a small hole made in apex, followed by an overnight post-fixation in 4% PFA at 4°C on a rocking platform. The specimens were prepared

with a rapid decalcification by 10% EDTA in PBS using a microwave Histos 5 (Milestone) during 4 to 6 h. All labeling incubations were carried out at 37°C, with agitation during 3 to 5 days, and then staining with a nucleic labeling with DAPI (Sigma) and washed in PBS. Each cochlea was transferred into a mounting solution X-clarity, stuck with glue at the bottom of a chamber for imaging. To image from macro view to cellular resolution and perform the 3D reconstruction, a Lavision BioTec UltraMicroscope II was used with a Clarity objective Plan-Neofluar 20×/1.0 immersion in a refractive index of 1.46. The Imaris 8.4.1 software was used to process three-dimensional acquisitions.

Image Acquisition

Specimens were examined with a Zeiss confocal microscope LSM 710 NLO Zeiss and fluorescent microscope Eclipse E800 Nikon. Quantification of grafted cells were performed on whole-mount cochlear epithelia. The nucleus of every cell (DAPI) surrounded by Dil signal visualized by fluorescence microscope Eclipse E800 Nikon was considered a Vybrant-Dil-positive cell. The distance (µm) of grafted cells within the cochlear sensory epithelium from basal membrane was determined from virtual slides of reconstituted 3D-cochlear images. For this analysis, overlapping images of cochlear sensory epithelium were acquired in Z stack by confocal microscope from basal membrane to reticular lamina (≈30 sections per whole-mount surface preparation at a distance of 1.52 µm). The analysis and images edition were performed with Zen software (Zeiss, Germany).

Statistical Analysis

At least three independent experiments were conducted for each determination, and data were expressed as mean ± standard error (SE). Statistical analysis is described at the end of the figure legends. Statistical difference was reported for p values less than 0.05.

SUPPLEMENTAL INFORMATION

Supplemental Information can be found online at <https://doi.org/10.1016/j.ymthe.2019.03.018>.

AUTHOR CONTRIBUTIONS

A.L.-J., H.L., and Y.C. performed experiments. A.L.-J., J.M.B., and A.Z. analyzed data. C.R. performed tissue-histoclearing and imaging. A.E. and Q.W. provided *Atoh1-GFP* cells and editing. A.Z. conceived the study, carried out experiments, analyzed data, and wrote the main manuscript text. All authors reviewed the manuscript.

CONFLICTS OF INTEREST

The authors declare no competing interests.

ACKNOWLEDGMENTS

We thank Prof B. Fritsch (University of Iowa) for critical reading of the manuscript. We thank Profs F. Féron and M. Khrestchatsky (Amu, France) for lab facilities and “La Fondation Pour l'Audition” (Paris, France) for a PhD fellowship rewarded to H.L. We thank the Experimental Histology Network of Montpellier for histology/immunohistology experiments (RHEM; <https://www.rhem.cnrs.fr/>). We

are grateful to all Otostem (<http://www.otostem.org>) partners for scientific discussions and suggestions. This project was sponsored by the EU-FP7 under the health topic, grant number 603029.

REFERENCES

- Agrup, C., Gleeson, M., and Rudge, P. (2007). The inner ear and the neurologist. *J. Neurol. Neurosurg. Psychiatry* 78, 114–122.
- Appler, J.M., and Goodrich, L.V. (2011). Connecting the ear to the brain: Molecular mechanisms of auditory circuit assembly. *Prog. Neurobiol.* 93, 488–508.
- Kelley, M.W. (2006). Regulation of cell fate in the sensory epithelia of the inner ear. *Nat. Rev. Neurosci.* 7, 837–849.
- Jahan, I., Pan, N., Elliott, K.L., and Fritzsche, B. (2015). The quest for restoring hearing: Understanding ear development more completely. *BioEssays* 37, 1016–1027.
- Corwin, J.T., and Cotanche, D.A. (1988). Regeneration of sensory hair cells after acoustic trauma. *Science* 240, 1772–1774.
- Ryals, B.M., and Rubel, E.W. (1988). Hair cell regeneration after acoustic trauma in adult Coturnix quail. *Science* 240, 1774–1776.
- Chardin, S., and Romand, R. (1995). Regeneration and mammalian auditory hair cells. *Science* 267, 707–711.
- Mathers, C.D., and Loncar, D. (2006). Projections of global mortality and burden of disease from 2002 to 2030. *PLoS Med.* 3, e442.
- Jongkamonwivat, N., Zine, A., and Rivolta, M.N. (2010). Stem cell based therapy in the inner ear: appropriate donor cell types and routes for transplantation. *Curr. Drug Targets* 11, 888–897.
- Zine, A., Lowenheim, H., and Fritzsche, B. (2014). Toward translating molecular ear development to generate hair cells from stem cells. In *Adult Stromal (Skeletal, Mesenchymal) Stem Cells: Advances Towards Clinical Applications*, Second Edition, K. Turksen, ed. (Springer), pp. 111–161.
- Warnecke, A., Mellott, A.J., Römer, A., Lenarz, T., and Staeker, H. (2017). Advances in translational inner ear stem cell research. *Hear. Res.* 353, 76–86.
- Ahmed, H., Shubina-Oleinik, O., and Holt, J.R. (2017). Emerging gene therapies for genetic hearing loss. *J. Assoc. Res. Otolaryngol.* 18, 649–670.
- Wang, L., Kempton, J.B., and Brigande, J.V. (2018). Gene therapy in mouse models of deafness and balance dysfunction. *Front. Mol. Neurosci.* 11, 300.
- Miwa, T., Minoda, R., Ise, M., Yamada, T., and Yumoto, E. (2013). Mouse otocyst transuterine gene transfer restores hearing in mice with connexin 30 deletion-associated hearing loss. *Mol. Ther.* 21, 1142–1150.
- Lentz, J.J., Jodelka, F.M., Hinrich, A.J., McCaffrey, K.E., Farris, H.E., Spalitta, M.J., Bazan, N.G., Duelli, D.M., Rigo, F., and Hastings, M.L. (2013). Rescue of hearing and vestibular function by antisense oligonucleotides in a mouse model of human deafness. *Nat. Med.* 19, 345–350.
- Pan, B., Askew, C., Galvin, A., Heman-Ackah, S., Asai, Y., Indzhykilian, A.A., Jodelka, F.M., Hastings, M.L., Lentz, J.J., Vandenbergh, L.H., et al. (2017). Gene therapy restores auditory and vestibular function in a mouse model of Usher syndrome type 1c. *Nat. Biotechnol.* 35, 264–272.
- Olivius, P., Alexandrov, L., Miller, J., Ulfendahl, M., Bagger-Sjöbäck, D., and Kozlova, E.N. (2003). Allografted fetal dorsal root ganglion neuronal survival in the guinea pig cochlea. *Brain Res.* 979, 1–6.
- Hildebrand, M.S., Dahl, H.H., Hardman, J., Coleman, B., Shepherd, R.K., and de Silva, M.G. (2005). Survival of partially differentiated mouse embryonic stem cells in the scala media of the guinea pig cochlea. *J. Assoc. Res. Otolaryngol.* 6, 341–354.
- Tateya, I., Nakagawa, T., Iguchi, F., Kim, T.S., Endo, T., Yamada, S., Kageyama, R., Naito, Y., and Ito, J. (2003). Fate of neural stem cells grafted into injured inner ears of mice. *Neuroreport* 14, 1677–1681.
- Nishimura, K., Nakagawa, T., Sakamoto, T., and Ito, J. (2012). Fates of murine pluripotent stem cell-derived neural progenitors following transplantation into mouse cochleae. *Cell Transplant.* 21, 763–771.
- Parker, M.A., Corliss, D.A., Gray, B., Anderson, J.K., Bobbin, R.P., Snyder, E.Y., and Cotanche, D.A. (2007). Neural stem cells injected into the sound-damaged cochlea migrate throughout the cochlea and express markers of hair cells, supporting cells, and spiral ganglion cells. *Hear. Res.* 232, 29–43.
- Matsuoka, A.J., Kondo, T., Miyamoto, R.T., and Hashino, E. (2007). Enhanced survival of bone-marrow-derived pluripotent stem cells in an animal model of auditory neuropathy. *Laryngoscope* 117, 1629–1635.
- Pandit, S.R., Sullivan, J.M., Egger, V., Borecki, A.A., and Oleskevich, S. (2011). Functional effects of adult human olfactory stem cells on early-onset sensorineural hearing loss. *Stem Cells* 29, 670–677.
- Corrales, C.E., Pan, L., Li, H., Liberman, M.C., Heller, S., and Edge, A.S. (2006). Engraftment and differentiation of embryonic stem cell-derived neural progenitor cells in the cochlear nerve trunk: growth of processes into the organ of Corti. *J. Neurobiol.* 66, 1489–1500.
- Chen, W., Jongkamonwivat, N., Abbas, L., Eshtan, S.J., Johnson, S.L., Kuhn, S., Milo, M., Thurlow, J.K., Andrews, P.W., Marcotti, W., et al. (2012). Restoration of auditory evoked responses by human ES-cell-derived otic progenitors. *Nature* 490, 278–282.
- Takahashi, K., Tanabe, K., Ohnuki, M., Narita, M., Ichisaka, T., Tomoda, K., and Yamanaka, S. (2007). Induction of pluripotent stem cells from adult human fibroblasts by defined factors. *Cell* 131, 861–872.
- Ealy, M., Ellwanger, D.C., Kosaric, N., Stapper, A.P., and Heller, S. (2016). Single-cell analysis delineates a trajectory toward the human early otic lineage. *Proc. Natl. Acad. Sci. USA* 113, 8508–8513.
- Koehler, K.R., Nie, J., Longworth-Mills, E., Liu, X.P., Lee, J., Holt, J.R., and Hashino, E. (2017). Generation of inner ear organoids containing functional hair cells from human pluripotent stem cells. *Nat. Biotechnol.* 35, 583–589.
- Lahlou, H., Lopez-Juarez, A., Fontbonne, A., Nivet, E., and Zine, A. (2018). Modeling human early otic sensory cell development with induced pluripotent stem cells. *PLoS ONE* 13, e0198954.
- Schilder, A.G.M., Blackshaw, H., Lenarz, T., Warnecke, A., Lustig, L.R., and Staeker, H. (2018). Biological Therapies of the Inner Ear: What Otolologists Need to Consider. *Otol. Neurotol.* 39, 135–137.
- Oesterle, E.C., Campbell, S., Taylor, R.R., Forge, A., and Hume, C.R. (2008). Sox2 and JAGGED1 expression in normal and drug-damaged adult mouse inner ear. *J. Assoc. Res. Otolaryngol.* 9, 65–89.
- Lang, H., Schulte, B.A., Goddard, J.C., Hedrick, M., Schulte, J.B., Wei, L., and Schmiedt, R.A. (2008). Transplantation of mouse embryonic stem cells into the cochlea of an auditory-neuropathy animal model: effects of timing after injury. *J. Assoc. Res. Otolaryngol.* 9, 225–240.
- Park, Y.H., Wilson, K.F., Ueda, Y., Tung Wong, H., Beyer, L.A., Swiderski, D.L., Dolan, D.F., and Raphael, Y. (2014). Conditioning the cochlea to facilitate survival and integration of exogenous cells into the auditory epithelium. *Mol. Ther.* 22, 873–880.
- Zhao, L.D., Li, L., Wu, N., Li, D.K., Ren, L.L., Guo, W.W., Sun, J.H., Liu, H.Z., Chen, Z.T., Xing, G.Q., and Yang, S.M. (2013). Migration and differentiation of mouse embryonic stem cells transplanted into mature cochlea of rats with aminoglycoside-induced hearing loss. *Acta Otolaryngol.* 133, 136–143.
- Coleman, B., Hardman, J., Coco, A., Epp, S., de Silva, M., Crook, J., and Shepherd, R. (2006). Fate of embryonic stem cells transplanted into the deafened mammalian cochlea. *Cell Transplant.* 15, 369–380.
- Backhouse, S., Coleman, B., and Shepherd, R. (2008). Surgical access to the mammalian cochlea for cell-based therapies. *Exp. Neurol.* 214, 193–200.
- Chen, J., and Streit, A. (2013). Induction of the inner ear: stepwise specification of otic fate from multipotent progenitors. *Hear. Res.* 297, 3–12.
- Weir, C., Morel-Kopp, M.C., Gill, A., Tinworth, K., Ladd, L., Hunyor, S.N., and Ward, C. (2008). Mesenchymal stem cells: isolation, characterisation and in vivo fluorescent dye tracking. *Heart Lung Circ.* 17, 395–403.
- Mortensen, L.J., Levy, O., Phillips, J.P., Stratton, T., Triana, B., Ruiz, J.P., Gu, F., Karp, J.M., and Lin, C.P. (2013). Quantification of Mesenchymal Stem Cell (MSC) delivery to a target site using in vivo confocal microscopy. *PLoS ONE* 8, e78145.
- Fuentes-Santamaría, V., Alvarado, J.C., Melgar-Rojas, P., Gabaldón-Ull, M.C., Miller, J.M., and Juiz, J.M. (2017). The Role of Glia in the Peripheral and Central Auditory System Following Noise Overexposure: Contribution of TNF- α and IL-1 β to the Pathogenesis of Hearing Loss. *Front. Neuroanat.* 11, 9.

41. Ladrech, S., Wang, J., Simonneau, L., Puel, J.L., and Lenoir, M. (2007). Macrophage contribution to the response of the rat organ of Corti to amikacin. *J. Neurosci. Res.* 85, 1970–1979.
42. Fredelius, L., and Rask-Andersen, H. (1990). The role of macrophages in the disposal of degeneration products within the organ of Corti after acoustic overstimulation. *Acta Otolaryngol.* 109, 76–82.
43. O'Malley, J.T., Nadol, J.B., Jr., and McKenna, M.J. (2016). Anti CD163+, Iba1+, and CD68+ cells in the adult human inner ear: Normal distribution of an unappreciated class of macrophages/microglia and implications for inflammatory otopathology in humans. *Otol. Neurotol.* 37, 99–108.
44. Liu, W., Molnar, M., Garnham, C., Benav, H., and Rask-Andersen, H. (2018). Macrophages in the human cochlea: saviors or predators-A study using super-resolution immunohistochemistry. *Front. Immunol.* 9, 223.
45. MacDonald, G.H., and Rubel, E.W. (2008). Three-dimensional imaging of the intact mouse cochlea by fluorescent laser scanning confocal microscopy. *Hear. Res.* 243, 1–10.
46. Abboud, N., Fontbonne, A., Watabe, I., Tonetto, A., Brezun, J.M., Feron, F., and Zine, A. (2017). Culture conditions have an impact on the maturation of traceable, transplantable mouse embryonic stem cell-derived otic progenitor cells. *J. Tissue Eng. Regen. Med.* 11, 2629–2642.
47. McLean, W.J., Yin, X., Lu, L., Lenz, D.R., McLean, D., Langer, R., Karp, J.M., and Edge, A.S.B. (2017). Clonal Expansion of Lgr5-Positive Cells from Mammalian Cochlea and High-Purity Generation of Sensory Hair Cells. *Cell Rep.* 18, 1917–1929.
48. West, E.L., Gonzalez-Cordero, A., Hippert, C., Osakada, F., Martinez-Barbera, J.P., Pearson, R.A., Sowden, J.C., Takahashi, M., and Ali, R.R. (2012). Defining the integration capacity of embryonic stem cell-derived photoreceptor precursors. *Stem Cells* 30, 1424–1435.
49. Mandai, M., Homma, K., Okamoto, S., Yamada, C., Nomori, A., and Takahashi, M. (2012). Adequate Time Window and Environmental Factors Supporting Retinal Graft Cell Survival in rd Mice. *Cell Med.* 4, 45–54.
50. Ohyama, K., Salt, A.N., and Thalmann, R. (1988). Volume flow rate of perilymph in the guinea-pig cochlea. *Hear. Res.* 35, 119–129.
51. Wang, Q., Hu, X., Kim, H., Squatrito, M., Scarpace, L., deCarvalho, A.C., Lyu, S., Li, P., Li, Y., Barthel, F., et al. (2017). Tumor Evolution of Glioma-Intrinsic Gene Expression Subtypes Associates with Immunological Changes in the Microenvironment. *Cancer Cell* 32, 42–56.e6.
52. Okano, T., Nakagawa, T., Kita, T., Kada, S., Yoshimoto, M., Nakahata, T., and Ito, J. (2008). Bone marrow-derived cells expressing Iba1 are constitutively present as resident tissue macrophages in the mouse cochlea. *J. Neurosci. Res.* 86, 1758–1767.
53. Hirose, K., Discolo, C.M., Keasler, J.R., and Ransohoff, R. (2005). Mononuclear phagocytes migrate into the murine cochlea after acoustic trauma. *J. Comp. Neurol.* 489, 180–194.
54. Warchol, M.E., Schwendener, R.A., and Hirose, K. (2012). Depletion of resident macrophages does not alter sensory regeneration in the avian cochlea. *PLoS ONE* 7, e51574.
55. Sato, E., Shick, H.E., Ransohoff, R.M., and Hirose, K. (2008). Repopulation of cochlear macrophages in murine hematopoietic progenitor cell chimeras: the role of CX3CR1. *J. Comp. Neurol.* 506, 930–942.
56. Dinh, C.T., Goncalves, S., Bas, E., Van De Water, T.R., and Zine, A. (2015). Molecular regulation of auditory hair cell death and approaches to protect sensory receptor cells and/or stimulate repair following acoustic trauma. *Front. Cell. Neurosci.* 9, 96.
57. Matsuoka, A.J., Kondo, T., Miyamoto, R.T., and Hashino, E. (2006). In vivo and in vitro characterization of bone marrow-derived stem cells in the cochlea. *Laryngoscope* 116, 1363–1367.
58. Sharif, S., Nakagawa, T., Ohno, T., Matsumoto, M., Kita, T., Riazuddin, S., and Ito, J. (2007). The potential use of bone marrow stromal cells for cochlear cell therapy. *Neuroreport* 18, 351–354.
59. Schulze, J., Kaiser, O., Paasche, G., Lamm, H., Pich, A., Hoffmann, A., Lenarz, T., and Warnecke, A. (2017). Effect of hyperbaric oxygen on BDNF-release and neuroprotection: Investigations with human mesenchymal stem cells and genetically modified NIH3T3 fibroblasts as putative cell therapeutics. *PLoS ONE* 12, e0178182.
60. Hu, Z., Andäng, M., Ni, D., and Ulfendahl, M. (2005). Neural co-graft stimulates the survival and differentiation of embryonic stem cells in the adult mammalian auditory system. *Brain Res.* 1051, 137–144.
61. Sullivan, J.M., Cohen, M.A., Pandit, S.R., Sahota, R.S., Borecki, A.A., and Oleskevich, S. (2011). Effect of epithelial stem cell transplantation on noise-induced hearing loss in adult mice. *Neurobiol. Dis.* 41, 552–559.